Editors' Suggestion

# Tailoring band structure and band filling in a simple cubic (IV, III)-VI superconductor

M. Kriener,[1,*] M. Kamitani,[1] T. Koretsune,[1,2] R. Arita,[1] Y. Taguchi,[1] and Y. Tokura[1,3]

[1]*RIKEN Center for Emergent Matter Science (CEMS), Wako 351-0198, Japan*

[2]*Department of Physics, Tohoku University, Miyagi 980-8578, Japan*

[3]*Department of Applied Physics and Quantum-Phase Electronics Center (QPEC), University of Tokyo, Tokyo 113-8656, Japan*

(Received 14 January 2018; published 25 April 2018)

Superconductivity and its underlying mechanisms are one of the most active research fields in condensed-matter physics. An important question is how to enhance the transition temperature $T_c$ of a superconductor. In this respect, the possibly positive role of valence-skipping elements in the pairing mechanism has been attracting considerable interest. Here we follow this pathway and successfully enhance $T_c$ up to almost 6 K in the simple chalcogenide SnTe known as a topological crystalline insulator by doping the valence-skipping element In substitutionally for the Sn site and codoping Se for the Te site. A high-pressure synthesis method enabled us to form single-phase solid solutions $Sn_{1-x}In_xTe_{1-y}Se_y$ over a wide composition range while keeping the cubic structure necessary for the superconductivity. Our experimental results are supported by density-functional theory calculations which suggest that even higher $T_c$ values would be possible if the required doping range was experimentally accessible.

DOI: 10.1103/PhysRevMaterials.2.044802

## I. INTRODUCTION

Narrow-gap chalcogenide semiconductors, such as GeTe, PbTe, or $Bi_2Se_3$ have attracted long-lasting interest due to their surprisingly rich variety on physical properties given their chemical simplicity. Also, the abundance of interesting features can be greatly enhanced by substitutional doping. In recent years, this class of materials has become even better known since many among them were found to host topological insulator phases of matter where the bulk is insulating whereas the surface allows metallic conduction owing to a peculiar band structure and strong spin-orbit interaction [1–3]. One prominent example is SnTe, which was predicted and soon after experimentally verified to be a topological crystalline insulator [4,5] where the topological nontrivial band structure is protected by the mirror symmetry of the underlying crystal structure [6]. SnTe, or more precisely $Sn_{1-\delta}Te$, is also a self-doped superconductor with a superconducting transition temperature of $T_c < 300$ mK [7]. However when doping In, $T_c$ is enhanced by one order of magnitude [8–10].

This enhancement and the discovery of the topological nature of SnTe have generated considerable interest in this system in recent years [11–20]. A zero-bias conduction peak was found in point-contact spectroscopy experiments on $Sn_{1-x}In_xTe$ at low doping $x \approx 0.045$ [11]. In addition, angle-resolved photoemission spectroscopy measurements confirmed that the topological band structure survives against the doping [12], and it was concluded that $Sn_{1-x}In_xTe$ is a promising candidate to realize topological superconductivity where the superconducting gap function possesses a nontrivial topology. By contrast, a recent nuclear-magnetic-resonance study on similarly low-doped $Sn_{1-x}In_xTe$ suggests conventional superconductivity [20].

All these works focus on $x \leqslant 0.5$, which is the solubility limit of In in cubic SnTe at ambient conditions. The end member InTe is a tetragonal semiconductor and does not superconduct. However, when synthesizing InTe under a pressure of $p \sim 3$ GPa, cubic InTe with rock-salt structure forms and is metastable at room temperature. Moreover it superconducts below $T_c \sim 3$ K [21,22], motivating, in this paper, to synthesize $Sn_{1-x}In_xTe$ for $x \geqslant 0.5$ and their Se-codoped analogs by employing a high-pressure synthesis method.

Polycrystalline samples of $Sn_{1-x}In_xTe_{1-y}Se_y$ with $x \geqslant 0.5$ were prepared by a high-pressure technique at 5 GPa and 1200–1300 °C. Throughout the paper, $x$ and $y$ denote nominal compositions. From the observed lattice parameter change obeying Vegard's law, the $x$ and $y$ values are anticipated to represent the actual In and Se contents, respectively, in the synthesized compounds with no discernible impurity phase. For comparison, we also synthesized samples for $x < 0.5$ by conventional melt growth and confirmed quantitative agreement with the results found in literature, e.g., that $T_c$ increases roughly linearly for $0.1 < x < 0.5$ [13–20]. The synthesis conditions are comparatively summarized in Table S1 and results of powder x-ray diffraction measurements for selected samples in Fig. S1 along with estimated lattice constants in Figs. S2 and S3 in the Supplemental Material [23]. Resistivity and specific heat were measured in a commercially available system (physical property measurement system, Quantum Design) by a standard four-probe technique and a relaxation method, respectively. The superconducting $T_c$ is defined as the temperature where zero resistance is achieved. In specific-heat data, the onset temperature of the superconducting jump is adopted as $T_c$. The electronic structures, phonon frequencies, and electron-phonon couplings were calculated in the framework of the density-functional theory (DFT) and the density-functional perturbation theory as implemented in the QUANTUM-ESPRESSO package [24]. Then, theoretical $T_c$ values were obtained using the McMillan-Allen-Dynes formula [25]. For details, see Sec. S6 in the Supplemental Material [23].

*Corresponding author: markus.kriener@riken.jp

 

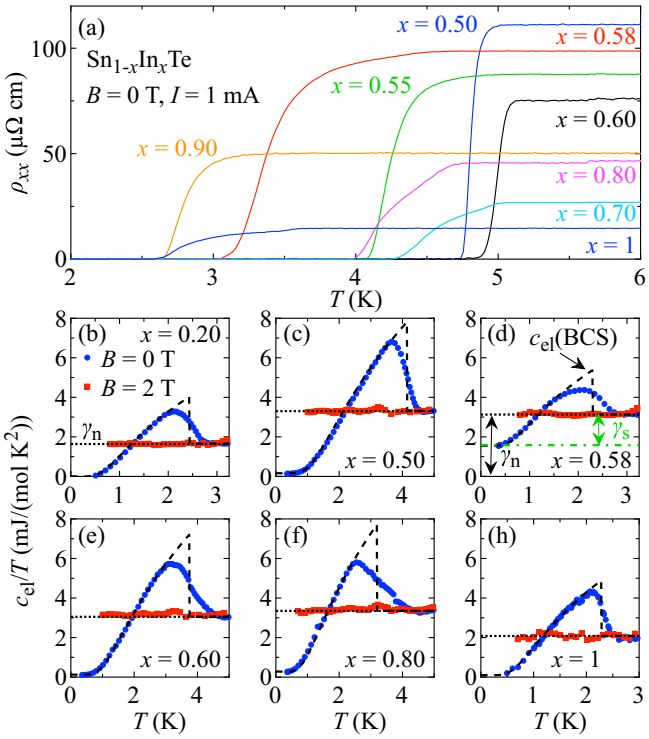


FIG. 1. (a) Temperature-dependent resistivity data of selected samples $0.5 \leqslant x \leqslant 1$. (b)–(h) Electronic specific-heat data $c_{el}/T$ in $B = 0$ T (blue data; circles) and 2 T (red; squares) are plotted against temperature ($T$) for selected samples $0.2 \leqslant x \leqslant 1$. A magnetic field of 2 T is sufficient to suppress the superconductivity in this system. The black dotted lines denote the electronic specific-heat coefficient of the normal-state $\gamma_n$. The green dashed-dotted line in (d) indicates the residual DOS, and its difference to $\gamma_n$ corresponds to the superconducting density of states $\gamma_s$ (not shown for the other samples, see text). The dashed lines are modeled BCS electronic specific heat, see Sec. S5 in the Supplemental Material [23] for details.

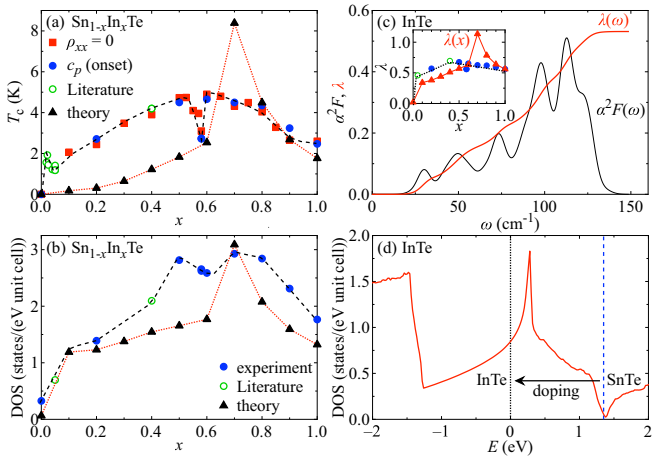


FIG. 2. (a) Superconducting $T_c$ vs In concentration $x$: The red data points (squares) correspond to the temperatures at which zero resistance is achieved, the blue data points (filled circles) correspond to the onset temperatures of the jumplike anomaly in specific-heat data, and the black data points (triangles) are calculated $T_c$ values. (b) DOS vs $x$: The blue data points (filled circles) were estimated from the experimental electronic specific-heat coefficient $\gamma_n$, and the black data points (triangles) are theoretical DOS values (see text for details). The green data points (open circles) in (a) and (b) are taken from literature (Refs. [13,19]) for comparison. The dashed and dotted lines in both panels are guides to the eyes. (c) Calculated Eliashberg function $\alpha^2 F$ (black) and (integrated) electron-phonon coupling constant $\lambda$ (red) as a function of the phonon frequency $\omega$ for InTe. The inset shows the $x$ dependence of calculated $\lambda$ values (red triangles connected with a solid line) compared with those estimated from specific-heat data (blue filled circles). The green data points (open circles) are taken from Ref. [19]. (d) Calculated DOS for InTe as a function of energy. The Fermi energy $E_F$ of InTe is defined as 0 and indicated with a dotted line. The approximate position of $E_F$ of SnTe is highlighted with a blue dashed line. The arrow indicates the effect of In doping on $E_F$ in $Sn_{1-x}In_xTe$.

## II. RESULTS

Temperature-dependent resistivity $\rho_{xx}$ data of selected high-pressure grown samples of $Sn_{1-x}In_xTe$ ($0.5 \leqslant x \leqslant 1$) are summarized in Fig. 1(a). All examined materials exhibit superconducting transitions between 2 and 5 K. One remarkable feature is the unexpected and steep suppression of $T_c = T$ ($\rho_{xx} = 0$) in the narrow doping range around $x \approx 0.58$, which was confirmed to be quite reproducible for several samples from different synthesis runs. For $x = 0.525$ (data not shown), we find $T_c \approx 4.75$ K which decreases down to the minimum $T_c$ of 3.1 K for $x = 0.58$, amounting to a suppression of ~35%. Interestingly, $T_c$ adopts its maximum value 4.9 K for $y = 0$ at a merely slightly higher In concentration of $x = 0.6$. Upon further doping, $T_c$ monotonously decreases towards InTe.

Figures 1(b)–1(h) show superconducting and normal-state electronic specific-heat data $c_{el}$ of selected samples $0.2 \leqslant x \leqslant 1$ displayed as $c_{el}/T$ vs $T$ [blue data (circles): $B = 0$ T; red (squares): 2 T]. The dotted horizontal lines denote the respective electronic specific-heat (Sommerfeld) coefficients $\gamma_n$. The dashed lines represent the Bardeen-Cooper-Schrieffer (BCS) electronic specific heat for the experimental values of $T_c$ and $\gamma_s$ (see Sec. S5 in the Supplemental Material [23] for their exact definition and the details of the specific-heat analysis). Concurrently with the suppression of $T_c$, the superconducting volume fraction also decreases drastically to roughly 50% for $x = 0.58$ as indicated by the residual density of states (green dashed-dotted line) in Fig. 1(d). For all other samples the specific-heat analysis yielded superconducting volume fractions of 90–100%, indicating the bulk nature of the superconductivity in this system. We also find that $c_{el}$ can be satisfactorily described in a weak-coupling BCS scenario throughout the doping series as indicated by the dashed lines in each panel. However, at low-doping concentrations $x \leqslant 0.5$, the description is slightly better when assuming a more strong-coupling BCS scenario in agreement with earlier studies [13,19], see also Fig. S7 in the Supplemental Material [23]. Magnetization measurements also confirm large shielding signals (cf. Fig. S4 in the Supplemental Material [23]).

Figure 2(a) presents the superconducting phase diagram of $Sn_{1-x}In_xTe$ as determined from resistivity (zero resistance), specific heat [onset of the jumplike anomaly in $c_{el}(T)$], and theoretically calculated $T_c$ values. The green data points (open circles) are taken from literature (Refs. [13,19]) for

comparison. The experimental $T_c$ values exhibit a domelike $x$ dependence with a sharp diplike anomaly centered at $x = 0.58$.

In Fig. 2(b) the density of states (DOS) is shown against the In concentration $x$. For $x = 0$, we find experimentally a sizable DOS due to the unintentionally doped Sn vacancies giving rise to free charge carriers in otherwise semiconducting SnTe. Upon doping, the experimental DOS increases, exhibits a slight suppression around $x = 0.58$, and a maximum around $x = 0.7$. Towards InTe, the DOS decreases again.

Figure 2(d) shows the calculated DOS for InTe as a function of energy; the Fermi energy $E_F$ is taken as the origin (dotted vertical line). The approximate position of SnTe is indicated by a vertical dashed blue line in the rigid-band picture, showing the narrow-gap feature of SnTe. The arrow sketches the effect of In doping, i.e., the band-filling change. Our calculations yield a sharp peaklike anomaly above the Fermi level in InTe which is a van Hove singularity typically found for the rock-salt fcc structure. The effect of the van Hove singularity can also be traced on theoretical results for the DOS as a function of $x$ shown in Fig. 2(b). To readily compare our calculations with the experimental results, the theoretical DOS was corrected for the electron-phonon-interaction-induced enhancement of DOS data estimated from specific-heat measurements, cf. Sec. S6 in the Supplemental Material [23]. For $x = 0$, the calculated DOS is almost zero as expected for an insulator/semiconductor. Upon doping, the DOS increases and exhibits a maximum around $x = 0.7$. Towards InTe, the DOS decreases. Although the slight suppression in the experimental DOS around $x = 0.58$ is not seen in our calculated data, all other features are well reproduced, and there is a reasonable agreement between experimental and calculated DOS.

In Fig. 2(c) the calculated Eliashberg function $\alpha^2 F$ is plotted against the phonon frequency $\omega$ for the end compound InTe. The integration of $\alpha^2 F$ yields the electron-phonon coupling strength $\lambda$ which is plotted in red. The inset compares the $x$ dependence of theoretical (for $\omega \to \infty$) and experimental values of $\lambda$. Again, there is reasonable agreement between experiment and theory except the sizable enhancement in the calculated data around $x = 0.7$.

In the phase diagram in Fig. 2(a), we also show calculated $T_c$ values. At low doping the calculations qualitatively reproduce the overall tendency of increasing $T_c$ values with $x$, although the absolute values are not matching well. We note that spin-orbit interaction which is not included to the present calculations may account for at least a part of the discrepancy [26]. The maximum in $T_c$ is found around $x = 0.7$ which indicates the doping concentration where $E_F$ falls onto the van Hove singularity. Although the maximum $T_c$ value is overestimated in our DFT calculations, the quantitative agreement between experiment and theory is very good above $x \sim 0.7$.

We also performed DFT calculations for cubic InSe (reported to exist when grown at $\approx 10.4$ GPa [27]) to see whether Se codoping on the Te site can lead to a further enhancement of $T_c$ since lighter elements may generally yield higher phonon frequencies and hence higher $T_c$ values. The results are shown in Figs. 3(a) and 3(b) which contain the same information for InSe as Figs. 2(c) and 2(d) for InTe. Apparently, the integrated Eliashberg function shown in Fig. 3(a) yields an $\sim$2.5 times larger electron-phonon coupling constant $\lambda$ which may give rise to an increased pairing interaction. As shown

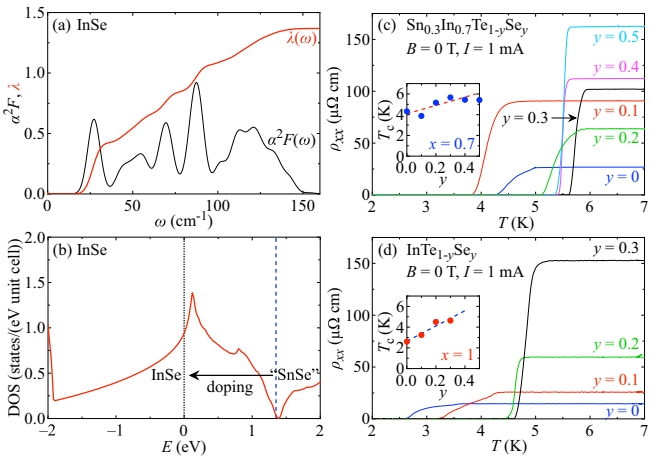


FIG. 3. (a) Calculated Eliashberg function $\alpha^2 F$ (black) and (integrated) electron-phonon coupling constant $\lambda$ (red) as a function of the phonon frequency $\omega$ for cubic InSe. (b) Calculated DOS for InSe as a function of energy. The Fermi energy $E_F$ of InSe is defined as 0 and indicated with a dotted line. The approximate position of $E_F$ of hypothetical "cubic SnSe" is highlighted with a blue dashed line. The arrow indicates the effect of In doping on $E_F$ in "cubic $Sn_{1-x}In_xSe$." (c) Resistivity data of codoped $Sn_{1-x}In_xTe_{1-y}Se_y$ for fixed $x = 0.7$ and (d) $x = 1$. The insets in both panels show the $y$ dependence of $T_c$.

in Fig. 3(b), the DOS of InSe exhibits a similar van Hove singularity as found in InTe. In InSe, the singularity lies closer to the Fermi level than in the case of InTe and explains why $\lambda$ is larger in InSe for which the present calculations predict $T_c = 8.5$ K. This suggests the experimental exploration at higher In concentrations for enhanced $T_c$ values by codoping Se.

Motivated by these DFT calculation results, we attempted to grow $Sn_{1-x}In_xTe_{1-y}Se_y$ crystals. This turned out to be possible up to $y = 0.5$ for $x = 0.5$–$0.7$ which is the solubility limit considering the applicable pressure range up to 8 GPa in our high-pressure apparatus. Resistivity data $\rho_{xx}$ for fixed $x = 0.7$ and $x = 1$ are shown in Figs. 3(c) and 3(d), respectively. Although the absolute values of the residual resistivities $\rho_{6\,K}$ systematically increase with $y$, all samples exhibit a drop to zero resistivity. The increase in $\rho_{6\,K}$ is likely a consequence of higher disorder in these samples due to the introduction of another dopant Se with different ionic size. Nevertheless, as suggested by our DFT calculations, $T_c$ is further enhanced. The inset in each panel shows $T_c$ vs the Se concentration $y$. The strongest enhancement was found for $x = 0.9$ and 1 where $T_c$ increases from $\sim$2.6 K for $y = 0$ to 4.6 and 5.0 K, respectively, for $y = 0.3$ which is the solubility limit for these high In concentrations. In the case of $x = 0.7$, $T_c$ increased from 2.6 K for $y = 0$ to 5.7 K for $y = 0.3$. The latter is the highest $T_c$ found in this paper. As can be seen in the inset of Fig. 3(c), the solubility limit for $x = 0.7$ is $y = 0.5$, but for this composition $T_c$ tends to slightly decrease again and saturate for higher Se concentrations. The $y$ dependence of other In concentrations $x$ can be found in Fig. S5 in the Supplemental Material [23]. There we also show in Fig. S3 the Se-codoping effect on the cubic lattice constant $a_c$ for $x = 0.7$ and $x = 1$. Due to the smaller ionic radius of Se, $a_c$ shrinks. Another way to compress the lattice is to apply physical pressure $p$. We probed

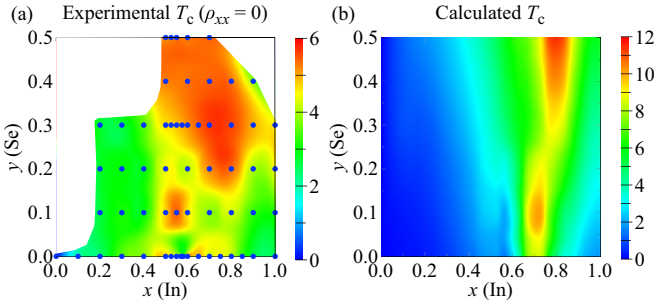


FIG. 4. (a) Experimentally and (b) theoretically determined superconducting phase diagrams of $Sn_{1-x}In_xTe_{1-y}Se_y$ as functions of $x$ and $y$. The blue symbols in (a) indicate the samples $(x, y)$ for which $T_c$ was actually measured. The white areas were not explored and are partially beyond the solubility limit for alloying $Sn_{1-x}In_xTe_{1-y}Se_y$. It should be noted that the scales in (a) and (b) differ by a factor of 2, therefore the color scheme is not the same in both panels.

this in the case of InTe: $T_c$ was found to decrease linearly as a function of $p$, see Fig. S6 in the Supplemental Material [23]. Such a behavior is often seen in conventional superconductors, and hence the $T_c$ enhancement by Se codoping is not due to the chemical pressure effect on the crystal lattice. This is in accord with our DFT calculations that the different characters of the wave functions when changing from $5p$ (Te) to $4p$ (Se) have a distinct effect on the pairing interaction.

Figures 4(a) and 4(b) provide a comparison between measured and calculated $T_c$ values of $Sn_{1-x}In_xTe_{1-y}Se_y$ as functions of $x$ and $y$. At low $x$, the DFT calculation systematically underestimates $T_c$. This is perhaps due to the rigid-band approximation and employing it to InTe and InSe rather than SnTe and hypothetic cubic SnSe, respectively. The real band structure may change upon doping beyond the rigid-band approximation. Nevertheless, the tendency towards enhanced $T_c$ values around $x \geqslant 0.6$ and $y \geqslant 0.3$ is correctly reproduced, and one can safely conclude that the optimal $x$ of the superconducting dome shifts towards $x = 1$ with increasing $y$.

## III. DISCUSSION

Finally, we discuss a possible scenario which can explain the observed features. Apparently, In and Se codoping into SnTe have the capability to increase $T_c$ from $<0.3$ K up to almost 6 K—or possibly even more with higher Se content. One scenario which attracted considerable interest in literature is the "negative-$U$ mechanism" which relies on valence-skipping elements [28–30]. Nominally In should replace Sn in an isovalent manner. However, the formal $In^{2+}$ state can be energetically unstable. In is then expected to appear as $In^{1+}$ ($4d^{10}5s^2$), $In^{3+}$ ($4d^{10}5s^0$), or even a mixture of them. Depending on the band filling, this may lead to, e.g., diamagnetic insulating or metallic behavior, a charge-Kondo effect, or possibly enhanced superconductivity [28–30]. Moreover, when the valence-skipping states order, a charge-density wave (CDW) can be expected. The negative-$U$ mechanism is, for example, considered to be responsible for the observed strong enhancements of $T_c$ in $Pb_{1-x}Tl_xTe$ and doped $BaBiO_3$ [31,32]. There is indeed support for the assumption that the In valence state plays a significant role in $Sn_{1-x}In_xTe$: A slope change in $T_c(x)$ was reported for $x \sim 0.08$–$0.1$ [19], which coincides with a change from hole doping (i.e., $In^{1+}$) to electron doping (i.e., $In^{3+}$) and with a slope change in the evolution of the cubic lattice constant when crossing $x \approx 0.1$, explainable with a change in the In valence states. Here we can only speculate about the origin of the enhancement of $T_c$ in $Sn_{1-x}In_xTe_{1-y}Se_y$. Spin-orbit interaction may play a role as well as the proposed In impurity band formation in $Sn_{1-x}In_xTe$, found in DFT calculations, which intersects the Fermi energy and consists of hybridized In-5$s$ and Te-5$p$ states [19]. However, assuming that the negative-$U$ mechanism is at least partially responsible for the enhancement of $T_c$ in $Sn_{1-x}In_xTe_{1-y}Se_y$, it is also possible to understand phenomenologically the sharp suppression of $T_c$ and superconducting volume fraction around $x = 0.58$ in $Sn_{1-x}In_xTe$. Such a dip structure of the superconducting phase diagram is sometimes encountered in unconventional systems, such as high-$T_c$ cuprates or iron pnictides. The doping concentration range where the superconductivity is suppressed is usually close to the onset of different orders and competing phases {e.g., stripe order (Ref. [33]) for $x \sim 0.125$ in $La_{2-x}Ba_xCuO_4$ or structural and magnetic order (Ref. [34]) for $x \sim 0.2$ in $LaFeAsO_{1-x}H_x$}. One may speculate that in $Sn_{1-x}In_xTe$ (and $Sn_{1-x}In_xTe_{1-y}Se_y$) a certain $In^{1+}$–$In^{3+}$ order forms out, e.g., a CDW supported by the apparent Fermi-surface instability at $x = 0.58$ and competes with the superconductivity. There might even be a critical $x$ value for which the superconductivity is completely suppressed. Slight chemical inhomogeneities may cause the 50% volume fraction and broaden the resistive transition as shown in Fig. 1(a). The very good quantitative agreement between experimental and calculated $T_c$ values in the highly doped region of the phase diagram [Fig. 2(a)] could then indicate that the negative-$U$ mechanism and thus the valence-skipping feature of In is of less importance for $x \geqslant 0.8$. The system (for $y = 0$) is simply metallic forming a conventional BCS superconductor at low temperatures as it is also supported by the physical-pressure effect on $T_c$. However, we could not find any experimental evidence yet for a CDW formation in $Sn_{1-x}In_xTe_{1-y}Se_y$ which could be a promising starting point for future works, such as site-selective-probe experiments and more elaborate theoretical work beyond DFT.

## IV. SUMMARY

To summarize, the full phase diagram of $Sn_{1-x}In_xTe$ for $0 \leqslant x \leqslant 1$ is reported and characterized by measurements of x-ray diffraction, resistivity, magnetization, and specific heat. The highest $T_c = 4.9$ K (zero resistivity) is found around $x = 0.6$. Interestingly just below this maximum there is a strong suppression of the superconductivity indicated by a sharp drop of the superconducting volume fraction to about 50% and $T_c$ to 3.1 K yielding a two-peak structure of the superconducting dome. By codoping Se into $Sn_{1-x}In_xTe_{1-y}Se_y$, $T_c$ was further enhanced to almost 6 K for $x = 0.7$ and $y = 0.3$, i.e., the superconducting dome shifts towards the In-rich side of the phase diagram. Our experimental findings are backed up by density-functional calculations. Observed discrepancies in the size of $T_c$ between theory and experiment for low-doped $Sn_{1-x}In_xTe$ indicate that additional mechanisms are at work being responsible for the observed enhancement of $T_c$ in this system. It is

speculated that the negative-$U$ mechanism due to the valence-skipping feature of In might explain the observed results.

## ACKNOWLEDGMENTS

The authors thank M. S. Bahramy for fruitful discussions and comments. This work was partly supported by Grants-in-Aid for Scientific Research (S) from the Japan Society for the Promotion of Science (JSPS, Grant No. 24224009), JST (Grant No. JP16H00924), PRESTO (Grant No. JPMJPR15N5), and Grants-in-Aid for Scientific Research (B) (JSPS, Grant No. 17H02770). M. Kriener was supported by a Grants-in-Aid for Scientific Research (C) (JSPS, Grant No. 15K05140).

M.K., M.K., and T.K. contributed equally to this work.

[1] M. Hasan and C. Kane, Rev. Mod. Phys. **82**, 3045 (2010).
[2] X.-L. Qi and S.-C. Zhang, Rev. Mod. Phys. **83**, 1057 (2011).
[3] Y. Ando and L. Fu, Annu. Rev. Condens. Matter Phys. **6**, 361 (2015).
[4] T. H. Hsieh, H. Lin, J. Liu, W. Duan, A. Bansil, and L. Fu, Nat. Commun. **3**, 982 (2012).
[5] Y. Tanaka, Z. Ren, T. Sato, K. Nakayama, S. Souma, T. Takahashi, K. Segawa, and Y. Ando, Nat. Phys. **8**, 800 (2012).
[6] L. Fu, Phys. Rev. Lett. **106**, 106802 (2011).
[7] R. A. Hein, J. W. Gibson, R. S. Allgaier, B. B. Houston, Jr., R. Mazelsky, and R. C. Miller, in *Proceedings of the 9th International Conference on Low Temperature Physics* (Plenum Press, New York, 1965), p. 604.
[8] T. Nakajima, M. Isino, H. Miyauchi, and E. Kanda, J. Phys. Soc. Jpn. **34**, 282 (1973).
[9] G. S. Bushmarina, I. A. Drabkin, V. V. Kompaniets, R. V. Parfen'ev, D. V. Shamshur, and M. A. Shakhov, Sov. Phys. Solid State **28**, 612 (1986).
[10] A. S. Erickson, J.-H. Chu, M. F. Toney, T. H. Geballe, and I. R. Fisher, Phys. Rev. B **79**, 024520 (2009).
[11] S. Sasaki, Z. Ren, A. A. Taskin, K. Segawa, L. Fu, and Y. Ando, Phys. Rev. Lett. **109**, 217004 (2012).
[12] T. Sato, Y. Tanaka, K. Nakayama, S. Souma, T. Takahashi, S. Sasaki, Z. Ren, A. A. Taskin, K. Segawa, and Y. Ando, Phys. Rev. Lett. **110**, 206804 (2013).
[13] M. Novak, S. Sasaki, M. Kriener, K. Segawa, and Y. Ando, Phys. Rev. B **88**, 140502(R) (2013).
[14] R. D. Zhong, J. A. Schneeloch, X. Y. Shi, Z. J. Xu, C. Zhang, J. M. Tranquada, Q. Li, and G. D. Gu, Phys. Rev. B **88**, 020505(R) (2013).
[15] L. P. He, Z. Zhang, J. Pan, X. C. Hong, S. Y. Zhou, and S. Y. Li, Phys. Rev. B **88**, 014523 (2013).
[16] V. K. Maurya, Shruti, P. Srivastava, and S. Patnaik, Europhys. Lett. **108**, 37010 (2014).
[17] M. Saghir, J. A. T. Barker, G. Balakrishnan, A. D. Hillier, and M. R. Lees, Phys. Rev. B **90**, 064508 (2014).
[18] T. Hashimoto, K. Yada, M. Sato, and Y. Tanaka, Phys. Rev. B **92**, 174527 (2015).
[19] N. Haldolaarachchige, Q. Gibson, W. Xie, M. B. Nielsen, S. Kushwaha, and R. J. Cava, Phys. Rev. B **93**, 024520 (2016).
[20] S. Maeda, R. Hirose, K. Matano, M. Novak, Y. Ando, and G.-q. Zheng, Phys. Rev. B **96**, 104502 (2017).
[21] H. E. Bömmel, A. J. Darnell, W. F. Libby, B. R. Tittmann, and A. J. Yencha, Science **141**, 714 (1963).
[22] A. J. Darnell, A. J. Yencha, and W. F. Libby, Science **141**, 713 (1963).
[23] See Supplemental Material at http://link.aps.org/supplemental/10.1103/PhysRevMaterials.2.044802 for complementing data, which includes Refs. [35–44].
[24] P. Giannozzi, S. Baroni, N. Bonini, M. Calandra, R. Car, C. Cavazzoni, D. Ceresoli, G. L. Chiarotti, M. Cococcioni, I. Dabo *et al.*, J. Phys.: Condens. Matter **21**, 395502 (2009).
[25] P. B. Allen and R. C. Dynes, Phys. Rev. B **12**, 905 (1975).
[26] R. Heid, K.-P. Bohnen, I. Y. Sklyadneva, and E. V. Chulkov, Phys. Rev. B **81**, 174527 (2010).
[27] U. Schwarz, A. R. Goñi, K. Syassen, A. Cantarero, and A. Chevy, High Pressure Res. **8**, 396 (2007).
[28] C. Varma, Phys. Rev. Lett. **61**, 2713 (1988).
[29] M. Dzero and J. Schmalian, Phys. Rev. Lett. **94**, 157003 (2005).
[30] I. Hase, K. Yasutomi, T. Yanagisawa, K. Odagiri, and T. Nishio, Physica C (Amsterdam) **527**, 85 (2016).
[31] Y. Matsushita, H. Bluhm, T. H. Geballe, and I. R. Fisher, Phys. Rev. Lett. **94**, 157002 (2005).
[32] R. J. Cava, B. Batlogg, J. J. Krajewski, R. Farrow, L. W. Rupp, Jr., A. E. White, K. Short, W. F. Peck, and T. Kometani, Nature (London) **332**, 814 (1988).
[33] J. M. Tranquada, Physica B (Amsterdam) **407**, 1771 (2012).
[34] M. Hiraishi, S. Iimura, K. M. Kojima, J. Yamaura, H. Hiraka, K. Ikeda, P. Miao, Y. Ishikawa, S. Torii, M. Miyazaki *et al.*, Nat. Phys. **10**, 300 (2014).
[35] M. Kriener, Y. Maeno, T. Oguchi, Z.-A. Ren, J. Kato, T. Muranaka, and J. Akimitsu, Phys. Rev. B **78**, 024517 (2008).
[36] M. Kriener, K. Segawa, Z. Ren, S. Sasaki, and Y. Ando, Phys. Rev. Lett. **106**, 127004 (2011).
[37] M. Tinkham, *Introduction to Superconductivity*, 2nd ed. (McGraw-Hill Book Co.-Singapore, New York, 1996).
[38] W. McMillan, Phys. Rev. **167**, 331 (1968).
[39] B. Mühlschlegel, Z. Phys. **155**, 313 (1959).
[40] H. Padamsee, J. Neighbor, and C. Shiffman, J. Low Temp. Phys. **12**, 387 (1973).
[41] J. P. Perdew, K. Burke, and M. Ernzerhof, Phys. Rev. Lett. **77**, 3865 (1996).
[42] D. Vanderbilt, Phys. Rev. B **41**, 7892 (1990).
[43] A. A. Mostofi, J. R. Yates, G. Pizzi, Y.-S. Lee, I. Souza, D. Vanderbilt, and N. Marzari, Comput. Phys. Commun. **185**, 2309 (2014).
[44] T. Koretsune and R. Arita, Comput. Phys. Commun. **220**, 239 (2017).